ON THE POLARIZATION OF THE NON-VALENCE COMPONENTS IN THE PROTON

By E. Richter-Wąs

Institute of Physics, Jagellonian University, Cracow*

(Received February 14, 1984)

The polarization of the non-valence components of the proton is discussed. The spin-spin asymmetry in two different processes with polarized incoming protons is taken as a probe of the problem. The first is the Drell-Yan process which is calculated with next-to-leading corrections for models with polarized and unpolarized sea. The second is the direct photon production at large p_T, where at the Born level the gluon distribution plays a dominant rôle.

PACS numbers: 12.40.-y

1. Introduction

The physical problem we would like to discuss is the polarization of the non-valence components of protons. It seems to be very interesting to what extent the spin of the particle is given by the spin of its components. The simplest models assume that all of the proton's spin is carried out by the valence quarks. It works well if the spin effects in the scattering process are dominated by the valence contributions. It is therefore important to find and calculate a process where the non-valence components polarization plays a dominant role.

In this paper we concentrate on two processes with polarized protons in both beam and target.

The first is the Drell-Yan process [1] where the sea polarization seems to be very important [2]. This subject was briefly presented earlier [3], here we present some more details. The spin-spin asymmetry (initial-initial) is exactly zero in the leading order, provided the sea is unpolarized. We checked that this result approximately holds when higher order corrections are included. Consequently, any significant deviation of the asymmetry from zero means that the sea is polarized. To see how big this effect could be, we calculated also an example with assumed non zero sea polarization. The spin-spin asymmetry turns out to be quite large in this case.

* Address: Instytut Fizyki UJ, Reymonta 4, 30-059 Kraków, Poland.

The second process is the direct photon production [4] at large transverse momentum, where the gluon distribution plays a dominant role [5]. At the Born level the significant part of the spin-spin asymmetry comes from the gluon polarization and is exactly zero if gluons are unpolarized. One may see that this quantity depends little on the shape of the gluon distribution function, the crucial dependence being in the normalization of the gluons' spin.

These two processes considered together can give a more complete insight into the problem of the spin distribution among proton components.

The paper is arranged as follows. In the next Section the formalism for the Drell-Yan process is presented. Section 3 describes the results of the calculations. Section 4 gives the formalism for direct photon production at large p_T. The numerical results are presented in Section 5. Summary (Section 6) closes the paper.

2. $p_\uparrow p_\uparrow \to \mu^+\mu^- X$ *process*

The kinematics of the Drell-Yan process in a collision of two hadrons (protons) is depicted in Fig. 1. As usual

$$x = Q^2/2pq \quad \text{and} \quad t = \ln Q^2/\mu^2, \tag{1}$$

where Q^2 is the invariant mass-squared of the lepton pair, q is the photon momentum, p is the beam hadron momentum and μ is some arbitrary mass scale.

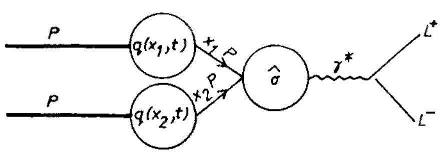

Fig. 1. Kinematical structure of the Drell-Yan process in a hadron-hadron collision

Hadron masses and constituent transverse momentum are neglected. For a polarized state of the hadron we deal with densities and helicity densities for quarks and the gluon respectively:

$$q(x) = q^+(x)+q^-(x), \qquad \Delta q(x) = q^+(x)-q^-(x),$$

$$G(x) = G^+(x)+G^-(x), \qquad \Delta G(x) = G^+(x)-G^-(x), \tag{2}$$

where + (−) denote the helicity parallel (antiparallel) to the helicity of the parent proton.

The evolution of the densities can be obtained from the Altarelli-Parisi equation [6] by a linear approximation

$$\frac{dq(x,t)}{dt} = \frac{q(x,t)-q(x,t_0)}{(t-t_0)} \tag{3}$$

and is given by

$$q_l(x,t) = q_l(x,t_0) + \frac{\alpha_s(t_0)}{2\pi}\int\limits_x^1 \frac{dy}{y}\left[P_{qq}\left(\frac{x}{y}\right) q_l(y,t_0) + P_{qG}\left(\frac{x}{y}\right) G(y,t_0)\right](t-t_0), \tag{4a}$$

$$G(x,t) = G(x,t_0) + \frac{\alpha_s(t_0)}{2\pi}\int\limits_x^1 \frac{dy}{y}\left[P_{Gq}\left(\frac{x}{y}\right)\sum_l q_l(y,t_0) + P_{GG}\left(\frac{x}{y}\right) G(y,t_0)\right](t-t_0), \tag{4b}$$

where [6]

$$P_{qq}(z) = \tfrac{4}{3}\left[\frac{(1+z^2)}{(1-z)_+} + \tfrac{3}{2}\,\delta(1-z)\right], \tag{5a}$$

$$P_{qG}(z) = \tfrac{1}{2}\,[z^2+(1-z)^2], \tag{5b}$$

$$P_{Gq}(z) = \tfrac{4}{3}\left[\frac{1+(1-z)^2}{z}\right], \tag{5c}$$

$$P_{GG}(z) = 6\left[\frac{z}{(1-z)_+} + \frac{1-z}{z} + z(1-z) + \tfrac{3}{4}\,\delta(1-z)\right], \tag{5d}$$

l is the flavour index, and t_0 is the evolution starting point. For helicity densities we have analogically [6]

$$\Delta q_l(x,t) = \Delta q_l(x,t_0) + \frac{\alpha_s(t_0)}{2\pi}\int\limits_x^1 \frac{dy}{y}$$

$$\times\left[\Delta P_{qq}\left(\frac{x}{y}\right)\Delta q_l(y,t_0) + \Delta P_{qG}\left(\frac{x}{y}\right)\Delta G(y,t_0)\right](t-t_0), \tag{6a}$$

$$\Delta G(x,t) = \Delta G(x,t_0) + \frac{\alpha_s(t_0)}{2\pi}\int\limits_x^1 \frac{dy}{y}$$

$$\times\left[\Delta P_{Gq}\left(\frac{x}{y}\right)\sum_l \Delta q_l(y,t_0) + \Delta P_{GG}\left(\frac{x}{y}\right)\Delta G(y,t_0)\right](t-t_0), \tag{6b}$$

where [6]

$$\Delta P_{qq}(z) = \tfrac{4}{3}\left[\frac{(1+z^2)}{(1-z)_+} + \tfrac{3}{2}\,\delta(1-z)\right], \tag{7a}$$

$$\Delta P_{qG}(z) = \tfrac{1}{2}\,[2z-1], \tag{7b}$$

$$\Delta P_{Gq}(z) = \tfrac{4}{3}\left[\frac{1-(1-z)^2}{z}\right], \tag{7c}$$

$$\Delta P_{GG}(z) = 3\left[(1+z^4)\left(\frac{1}{z} + \frac{1}{(1-z)_+}\right) - \frac{(1-z)^3}{z} + \tfrac{3}{2}\,\delta(1-z)\right]. \tag{7d}$$

One should be very careful when applying the linear approximation (4) and (6) to the solution of the master evolution equation for $t \gg t_0$ because it usually leads to the negative quark and gluon densities. In such case some iteration procedure is needed. Our results for the parton densities obtained by means of (4) and (6) agree with [7].

Defining the cross-section

$$\frac{d\sigma}{dQ^2} = \frac{1}{2}\left(\frac{d\sigma^{++}}{dQ^2} + \frac{d\sigma^{+-}}{dQ^2}\right) \tag{8a}$$

and the helicity cross-section

$$\frac{d\Delta\sigma}{dQ^2} = \frac{1}{2}\left(\frac{d\sigma^{++}}{dQ^2} - \frac{d\sigma^{+-}}{dQ^2}\right) \tag{8b}$$

where $\pm$ indices refer to the helicity of the incoming hadrons, we can express the initial--initial asymmetry as:

$$A_{ii} = \frac{d\Delta\sigma/dQ^2}{d\sigma/dQ^2} \,. \tag{9}$$

It can be written schematically (e.g. for quark-antiquark interactions)

$$A_{ii} = \frac{(\Delta q_i^{[1]}\Delta q_{\bar{i}}^{[2]})\otimes(\hat{\sigma}_{\uparrow\uparrow}-\hat{\sigma}_{\uparrow\downarrow})}{(q_i^{[1]}q_{\bar{i}}^{[2]})\otimes(\hat{\sigma}_{\uparrow\uparrow}+\hat{\sigma}_{\uparrow\downarrow})}\,, \tag{10}$$

where $\hat{\sigma}$ denotes the hard cross-section and the arrow up/down shows the parton helicity parallel/antiparallel to the hadron momentum. The symbol $\otimes$ stands for the appropriate integrations.

The Drell-Yan hard cross-section contains the graphs which are presented in Fig. 2.

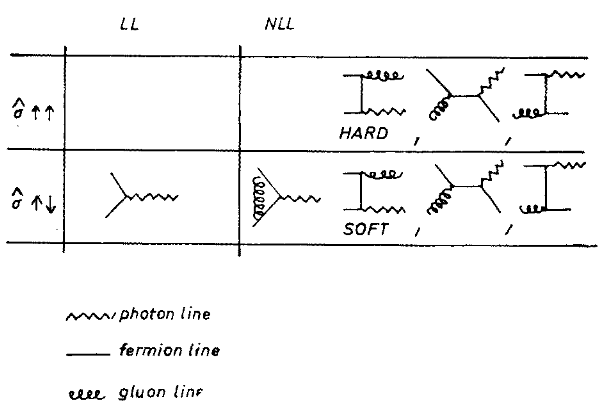

Fig. 2. The leading and next-to-leading order graphs for the Drell-Yan process. Arrow up/down shows the helicity parallel/antiparallel to the momentum

The lack of $\hat{\sigma}_{\uparrow\uparrow}$ in the leading-order is a simple consequence of the helicity conservation by vector interactions. The detailed formula in the $\alpha_s(Q^2)$ order reads [8]:

$$\frac{d\sigma}{dQ^2} = \frac{4\pi\alpha^2}{9SQ^2}\int\limits_0^1 \frac{dx_1}{x_1}\int\limits_0^1 \frac{dx_2}{x_2}\left\{\left[\sum_{l=1}^{f} e_l^2 q_l^{[1]}(x_1, t) q_{\bar{l}}^{[2]}(x_2, t) + (1\leftrightarrow 2)\right]\right.$$

$$\times\left[\delta(1-z) + \frac{\alpha_s(Q^2)}{2\pi}\,\theta(1-z)\,(f_{q,\mathrm{DY}}(z) - 2f_{q,2}(z))\right]$$

$$\left. + \left[\sum_{l=1}^{2f} e_l^2 q_l^{[1]}(x_1, t) G^{[2]}(x_2, t) + (1\leftrightarrow 2)\right]\frac{\alpha_s(Q^2)}{2\pi}\,\theta(1-z)\,(f_{G,\mathrm{DY}}(z) - f_{G,2}(z))\right\}, \quad (11)$$

where the next-to-leading order corrections are given by the differences [8]:

$$f_{q,\mathrm{DY}}(z) - 2f_{q,2}(z) = \tfrac{4}{3}\left[\frac{3}{(1-z)_+} + 2(1+z^2)\left(\frac{\ln(1-z)}{1-z}\right)_+ - 6 - 4z + \left(1 + \frac{4\pi^2}{3}\right)\delta(1-z)\right], \quad (12a)$$

$$f_{G,\mathrm{DY}}(z) - f_{G,2}(z) = \tfrac{1}{2}\left[z^2 + (1-z^2)\ln(1-z) + \frac{9z^2}{2} - 5z + \tfrac{3}{2}\right]. \quad (12b)$$

Analogically [9]

$$\frac{d\Delta\sigma}{dQ^2} = -\frac{4\pi\alpha^2}{9SQ^2}\int\limits_0^1 \frac{dx_1}{x_1}\int\limits_0^1 \frac{dx_2}{x_2}\left\{\left[\sum_{l/1}^{f} e_l^2 \Delta q_l^{[1]}(x_1, t)\Delta q_{\bar{l}}^{[2]}(x_2, t) + (1\leftrightarrow 2)\right]\right.$$

$$\left[\delta(1-z) + \frac{\alpha_s(Q^2)}{2\pi}\,\theta(1-z)\,(\Delta f_{q,\mathrm{DY}} - 2\Delta f_{q,2})\right]$$

$$\left. + \left[\sum_{l/1}^{2f} e_l^2 \Delta q_l^{[1]}(x_1, t)\Delta G^{[2]}(x_2, t) + (1\leftrightarrow 2)\right]\frac{\alpha_s(Q^2)}{2\pi}\,\theta(1-z)\,(\Delta f_{G,\mathrm{DY}} - \Delta f_G)\right\} \quad (13)$$

and [9]

$$\Delta f_{q,\mathrm{DY}}(z) - 2\Delta f_{q,2}(z) = (f_{q,\mathrm{DY}}(z) - 2f_{q,2}(z)) + \tfrac{4}{3}(2+2z), \quad (14a)$$

$$\Delta f_{G,\mathrm{DY}}(z) - \Delta f_G(z) = \tfrac{1}{2}\left[(2z-1)\ln(1-z) - \frac{3z^2}{2} + 3z - \tfrac{1}{2}\right]. \quad (14b)$$

$$\tau = Q^2/S, \qquad z = \tau/x_1x_2 = Q^2/s, \qquad s = x_1x_2S. \quad (15)$$

S is invariant mass-squared of the initial hadron system, s denotes the invariant mass--squared of the partonic subprocess.

3. *Numerical results*

In the leading order asymmetry A_{ii} is identically equal to zero if one assumes no sea polarization. This result nearly holds, if one takes into account the next-to-leading log corrections. In this order we have the contribution from the gluon polarization due to the appearance of the quark-gluon scattering graphs (in the numerator). These graphs, however, are small in comparison with the 3-point quark-antiquark-like diagrams (in the denominator), therefore, one can expect the spin-spin asymmetry to be close to zero.

These results are summarized in Fig. 3. In the leading order asymmetry is equal to zero. Curves A, B, C are the results of the calculation in the next-to-leading order with different

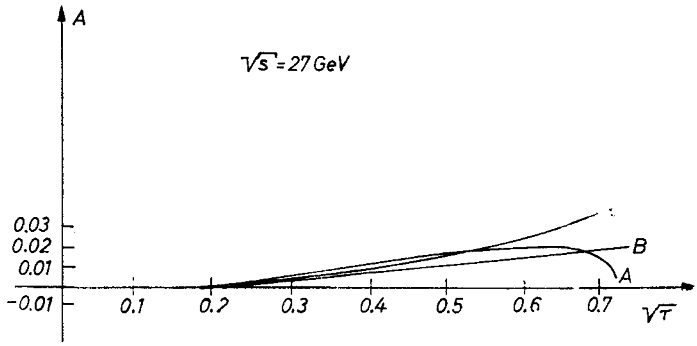

Fig. 3. The spin-spin asymmetry in the Drell-Yan process with unpolarized sea. In the leading order it is identically equal to zero. The solid line represents the next-to-leading order calculations. A, B, C are for different gluon distribution functions (described in Table I)

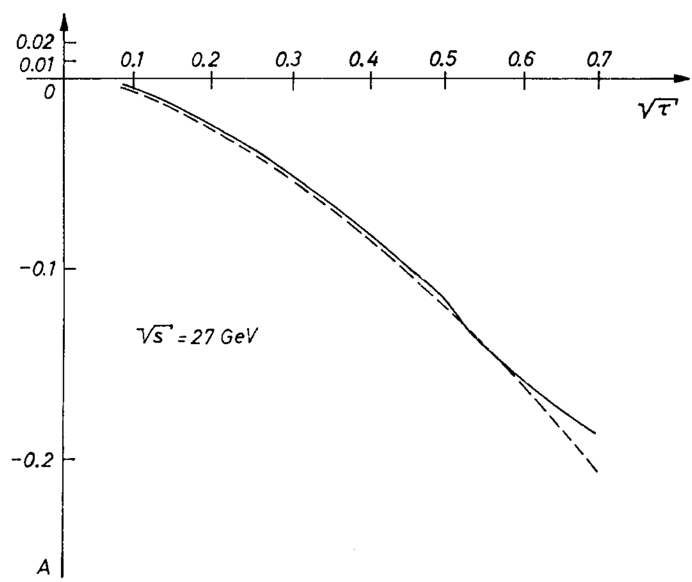

Fig. 4. The spin-spin asymmetry in the Drell-Yan process with polarized sea. The solid (broken) line shows the next-to-leading (leading) order calculations. Distribution functions are described in Table I

gluon distributions. The spin distributions and the parameters used in the calculations are described in the Appendix. We see that the spin-spin asymmetry does not exceed 3 per cent so one sees that the cancellation described above really takes place. One can also observe that the curves in Fig. 3 do not depend on the shape of the gluon distribution.

A dramatic change is observed when the sea polarization is introduced. The numerical results are drawn in Fig. 4. The asymmetry reaches the value of the 17–20% and is negative. We want to stress that the sea carrying only 3 per cent of the proton spin has changed the asymmetry by a factor of 6. Such modification of the sea spin (only 3 per cent of the proton's spin) can be hardly seen in most processes. Fig. 3 and 4 additionally supports the advantage of using the spin asymmetry. The large corrections which appear in the cross section and the helicity cross-section nearly cancel each other.

We conclude that any experiment which shows significant asymmetry in the Drell-Yan process clearly would indicate the existence of the sea polarization.

4. $p_\uparrow p_\uparrow \to \gamma X$ process at large p_T

At the Born level the cross-section and the helicity cross-section are dominated by the Compton scattering. The annihilation channel gives a much smaller contribution (we found it being on the level of few per cent of the Compton scattering) and thus it is neglected here.

The cross-section can be calculated according to the following formula [10]

$$E_\gamma \frac{d^3\sigma}{dp_\gamma^3} = \frac{s}{\pi} \int\limits_{x_{1\min}}^{1} dx_1 \frac{x_1 x_2}{x_1 s + u} \left[\sum_{l/1}^{2f} e_l^2 q_l^{[1]}(x_1, \ln Q^2/\mu^2) G^{[2]}(x_2, \ln Q^2/\mu^2) \right.$$

$$\left. \times \frac{d\hat{\sigma}}{d\hat{t}}(\mathrm{qG} \to \gamma \mathrm{q}) + G^{[1]}(x_1, \ln Q^2/\mu^2) \sum_{l/1}^{2f} e_l^2 q_l^{[2]}(x_2, \ln Q^2/\mu^2) \frac{d\hat{\sigma}}{d\hat{t}}(\mathrm{Gq} \to \gamma \mathrm{q}) \right]. \quad (16)$$

Similarly, for the helicity cross-section we obtain [10]:

$$E_\gamma \frac{d^3\Delta\sigma}{dp_\gamma^3} = \frac{s}{\pi} \int\limits_{x_{1\min}}^{1} dx_1 \frac{x_1 x_2}{x_1 s + u} \left[\sum_{l/1}^{2f} e_l^2 \Delta q_l^{[1]}(x_1, \ln Q^2/\mu^2) \Delta G^{[2]}(x_2, \ln Q^2/\mu^2) \right.$$

$$\left. \times \frac{d\Delta\hat{\sigma}}{d\hat{t}}(\mathrm{qG} \to \gamma \mathrm{q}) + \Delta G^{[1]}(x_1, \ln Q^2/\mu^2) \sum_{l/1}^{2f} e_l^2 \Delta q_l^{[2]}(x_2, \ln Q^2/\mu^2) \frac{d\Delta\hat{\sigma}}{d\hat{t}}(\mathrm{Gq} \to \gamma \mathrm{q}) \right]. \quad (17)$$

$$x_2 = -x_1 t/(x_1 s + u), \qquad x_{1\min} = -u/(s+t). \quad (18)$$

s, t, u are the c.m. Mandelstam variables for the proton-proton process; $\hat{s}$, $\hat{t}$, $\hat{u}$ are the c.m. Mandelstam variables for the parton subprocess

$$\hat{s} = x_1 x_2 s, \qquad \hat{t} = x_1 t, \qquad \hat{u} = x_2 u, \quad (19)$$

x_1, x_2 were defined in Section 2. In terms of the longitudinal and transverse momenta of the photon p_γ

$$x_F = 2p_{\gamma\|}/\sqrt{s} \quad \text{and} \quad x_T = 2p_{\gamma T}/\sqrt{s}. \tag{20}$$

One has

$$t = -\tfrac{1}{2}s(\sqrt{x_F^2+x_T^2}-x_F), \quad u = -\tfrac{1}{2}s(\sqrt{x_F^2+x_T^2}+x_F). \tag{21}$$

For the differential hard cross-section we have [9, 10]

$$\frac{d\hat{\sigma}}{d\hat{t}}(qG \to \gamma q) = -\tfrac{1}{6}\pi\alpha\alpha_s(Q^2)\frac{1}{\hat{s}^2}\left(\frac{\hat{t}}{\hat{s}}+\frac{\hat{s}}{\hat{t}}\right), \tag{22a}$$

$$\frac{d\Delta\hat{\sigma}}{d\hat{t}}(qG \to \gamma q) = -\tfrac{1}{6}\pi\alpha\alpha_s(Q^2)\frac{2}{\hat{s}^2}\left(-\frac{\hat{t}}{\hat{s}}+\frac{\hat{s}}{\hat{t}}\right). \tag{22b}$$

For $Gq \to \gamma q$ one has to replace $\hat{t}$ by $\hat{u}$.

The spin-spin asymmetry is defined as in Eq. (9).

It is not clear what value of Q^2 should be taken as the argument of the running coupling constant and the structure functions. For our choice of the gluon distribution the value $Q^2 = p_T^2$ seems to be the most suitable one [11, 12].

5. *Numerical results*

The asymmetry A_{ii} is identically zero at the Born level provided one assumes no gluon polarization. Figure 5 shows the calculated spin-spin asymmetry for three different gluon densities. Asymmetry does not depend upon the shape of the gluon distributions. Fig. 6 displays the curves which have been calculated for different distributions of spin among gluons and valence components. (The changes of the spin normalization satisfy

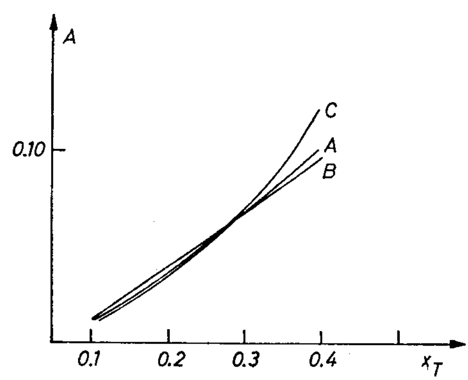

Fig. 5. The spin-spin asymmetry in direct photon production process for different gluon densities at the beam energy $\sqrt{s}$ = 63 GeV, x_F = 0. Distribution functions are described in Table II

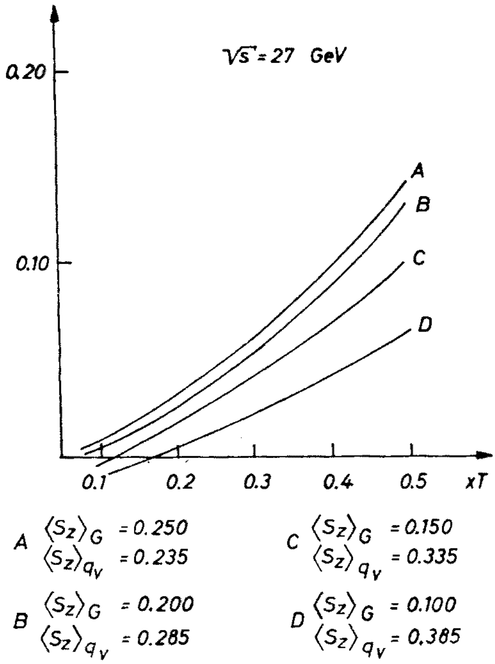

Fig. 6. The spin-spin asymmetry at $\sqrt{s}$ = 27 GeV and different normalizations of the gluon and the quark polarization density. Spin which is taken by the sea is fixed at the value of $\langle S_z \rangle_{sea}$ = .015. For distribution functions see Table II

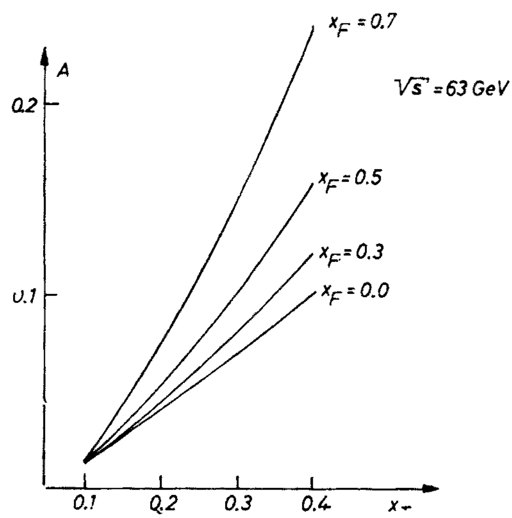

Fig. 7. The spin-spin asymmetry for direct photon production at $\sqrt{s}$ = 63 GeV and different values of x_F. For distribution functions see Table II

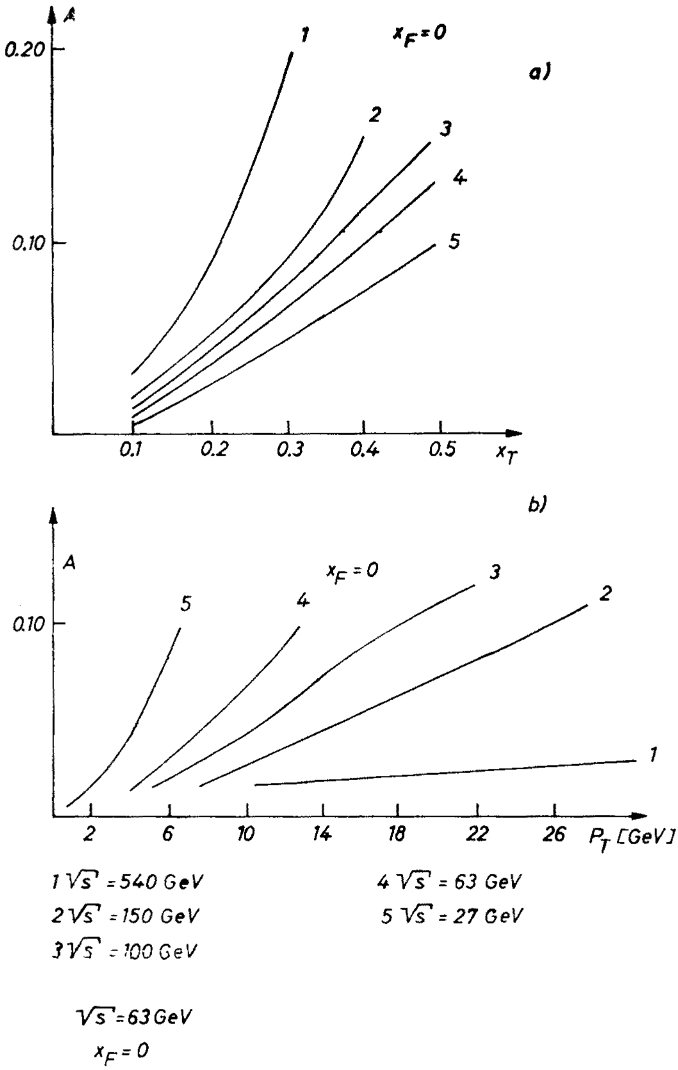

Fig. 8. The spin-spin asymmetry for direct photon production at $\sqrt{s}$ = 27 GeV, 63 GeV, 100 GeV, 150 GeV, 540 GeV, $x_F = 0$. For distribution functions see Table II

the Bjorken sum rule and keep the polarization of the sea fixed). The asymmetry increases with the spin carried by gluons and reaches the maximum value when the spin is distributed nearly equally between gluons and valence quarks.

Figs. 7, 8 show the dependence of the spin-spin asymmetry upon the kinematical variables and the beam energy. The asymmetry is growing with x_F and x_T (see Fig. 7). The increase in the beam energy decreases the asymmetry when the transverse momentum is fixed (Fig. 8a). With fixed x_T one can find that the asymmetry increases with the beam energy (Fig. 8b). This means that an increase in the scale Q^2 decreases the asymmetry.

6. *Summary*

In this paper we have proposed two processes with polarized incoming protons to test the problem of polarization of the non-valence hadron components: the Drell-Yan process for the sea polarization, and the direct photon production for the gluon polarization. The quantity which was found to be sensitive to this problem is the spin-spin asymmetry (initial-initial) (Eq. (9)).

1. For both processes asymmetry is equal identically to zero provided one assumes no non-valence component polarization. If one admits non-valence components being polarized, the situation changes dramatically. The asymmetry started to be quite large: for Drell-Yan process it reaches 17–20%, for direct photon production — 10–13%.

2. Each process tests the polarization of one non-valence component independently of the other one.

3. Drell-Yan spin-spin asymmetry depends strongly on the polarization of the sea. Let us stress that the sea carrying only 3% of the proton spin has changed the asymmetry by a factor of 6.

4. One may compare Fig. 5 and Fig. 6 and notice that the direct photon spin asymmetry depends very little on the shape of the gluon distribution and the gluon spin distribution and it seems to be dependent only on the spin normalization.

5. For the Drell-Yan process the large corrections which appear in the cross-section and the helicity cross-section nearly cancel in the helicity asymmetry. The problem of finding all corrections to direct photon production has not been worked out completely.

To conclude, we think that these two processes together may provide a good composite test for the problem of non-valence hadron components.

I am grateful to Dr. Jerzy Szwed for constant interest and many helpful remarks. I would like to thank Dr. Michał Praszałowicz and Dr. Maciej Nowak for useful suggestions.

APPENDIX

For valence quark distributions the Carlitz-Kaur model was adopted [13]. In this model the valence quarks carry most of the proton spin only for $x \to 1$. One introduces a spin dilution factor

$$\cos 2\theta = [1+0.052x^{-1/2}(1-x)^2]^{-1} \tag{1}$$

which becomes more important for small x. In this model the spin distributions for valence quarks are

$$\Delta u_v(x) = [u_v(x)-\tfrac{2}{3}\, d_v(x)] \cos 2\theta \tag{2a}$$

$$\Delta d_v(x) = -\tfrac{1}{3}\, d_v(x) \cos 2\theta \tag{2b}$$

which satisfy the Bjorken sum rule. In the Carlitz-Kaur approach the sea quarks are not polarized. The gluon and possible sea polarization were obtained from the bremsstrahlung model [14–15]. In this model the polarization of the sea quarks results because they

TABLE I

The quark and gluon densities at $Q_0^2 = 75\ \mathrm{GeV}^2$ used for Drell-Yan process calculations [13–15]

<table>
<tr><th></th><th>FIG. 3A</th><th>FIG. 3B</th><th>FIG. 3C</th><th>FIG. 4</th></tr>
<tr><td>$u_v(x)$</td><td colspan="4">$(1.433-0.433x)A_0/x$</td></tr>
<tr><td>$d_v(x)$</td><td colspan="4">$0.866(1-x)A_0/x$</td></tr>
<tr><td>$\Delta u_v(x)$</td><td colspan="4">$(u_v(x)-\frac{2}{3}d_v(x))\cos 2\theta$</td></tr>
<tr><td>$\Delta d_v(x)$</td><td colspan="4">$-1/3d_v(x)\cos 2\theta$</td></tr>
<tr><td>$\cos 2\theta$</td><td colspan="4">$1/(1+0.052(1-x)^2/\sqrt{x})$</td></tr>
<tr><td>A_0</td><td colspan="2">$3.0(1-x^2)^3\sqrt{x}\,(0.174+0.085(1-x^2)^2)/(0.58+0.43x)$</td><td colspan="2">$2.8(1-x^2)^3\sqrt{x}\,(0.174+0.085(1-x^2)^2)/(0.57+0.43x)$</td></tr>
<tr><td>$s(x)$</td><td colspan="2">$0.104(1-x)^7/x$</td><td colspan="2">$0.071(1-x)^8(1+(1-x)^2)/x$</td></tr>
<tr><td>$G(x)$</td><td>$3(1-x)^5/x$</td><td>$2.11(1+0.01(1-x)+0.02(1-x)^2$
$+0.1(1-x)^3)\,(1-x)^4/x$</td><td colspan="2">$2.05(1-x)^6(1+(1-x)^2)/x$</td></tr>
<tr><td>$\Delta S(x)$</td><td colspan="3">$\equiv 0$</td><td>$0.024(1-x)^8(1-(1-x)^2)/x$</td></tr>
<tr><td>$\Delta G(x)$</td><td>$0.2(1.67x-0.67x^2)G(x)$</td><td>$0.2(1.63x-0.63x^2)G(x)$</td><td colspan="2">$0.682(1-x)^6(1-(1-x)^2)/x$</td></tr>
</table>

TABLE II

The quark and gluon densities at $Q_0^2 = 75$ GeV^2 used for direct photon production calculations [13–15]

	FIG. 5B	FIG. 5A, 7, 8	FIG. 5C, 6
$u_v(x)$		$(1.433-0.433x)A_0/x$	
$d_v(x)$		$0.866(1-x)A_0/x$	
$\Delta u_v(x)$		$(u_v(x)-\frac{2}{3}d_v(x))\cos 2\theta$	
$\Delta d_v(x)$		$-\frac{1}{3}d_v(x)\cos 2\theta$	
A_0		$2.8(1-x^2)^3\sqrt{x}(0.174+0.085(1-x^2)^2)/(0.57+0.43x)$	
$\cos 2\theta$		$1/(1+0.052(1-x)^2/\sqrt{x})$	
$s(x)$		$0.071(1-x)^8(1+(1-x)^2)/x$	
$\Delta s(x)$		$0.024(1-x)^8(1-(1-x)^2)/x$	
$G(x)$	$3.12(1-x)^5/x$	$2.38(1+0.01(1-x)+0.02(1-x)^2 +0.1(1-x)^3)(1-x)^4/x$	$2.05(1-x)^6(1+(1-x)^2)/x$
$\Delta G(x)$	$0.22(1.67x-0.67x^2)G(x)$	$0.22(1.63x-0.63x^2)G(x)$	$0.682(1-x)^6(1-(1-x)^2)/x$

originate from gluons radiated by the valence quarks originally polarized. The detailed formulae for used distribution functions are given in Table I for the Drell-Yan process and in Table II for direct photon production.

The QCD running coupling constant was given by

$$\alpha_s(Q^2) = \frac{12\pi}{27 \ln Q^2/\Lambda^2} \tag{3}$$

where we took $\Lambda = 0.5$ GeV [8]. The starting point of the evolution of the structure functions was fixed at $Q_0^2 = 75$ GeV^2.

REFERENCES

[1] S. D. Drell, T. M. Yan, *Phys. Rev. Lett.* **25**, 316 (1970); *Ann. Phys.* (USA) **66**, 578 (1971).
[2] F. Close, D. Sivers, *Phys. Rev. Lett.* **39**, 1116 (1977).
[3] E. Richter-Wąs, J. Szwed, Cracow preprint 1983, TPJU-20/83.
[4] F. Halzen, D. M. Scott, *Phys. Rev. Lett.* **40**, 1117 (1978); *Phys. Rev.* **D18**, 3378 (1978).
[5] N. S. Craigie, ICTP, Trieste, pieprint IC/83/1.
[6] G. Altarelli, G. Parisi, *Nucl. Phys.* **B126**, 298 (1977).
[7] A. Buras, K. J. Gaemers, *Nucl. Phys.* **B132**, 249 (1978).
[8] G. Altarelli, R. K. Ellis, G. Martinelli, *Nucl. Phys.* **B157**, 461 (1979).
[9] P. Ratcliffe, *Nucl. Phys.* **B223**, 45–60 (1983).
[10] N. S. Craigie et al., *Nucl. Phys.* **B204**, 365–374 (1982).
[11] M. Nowak, M. Praszałowicz, *Z. Phys.* **C17**, 249–252 (1983).
[12] A. P. Contogouris, M. Sanielevici, CERN preprint 1983, Ref. TH-3656.
[13] J. Kaur, *Nucl. Phys.* **B128**, 219–251 (1977).
[14] N. S. Craigie et al., *Z. Phys.* **C12**, 173 (1982).
[15] J. Babcock, E. Monsay, D. Sivers, *Phys. Rev* **D19**, 1483 (1979).